Predicting the site-specific distribution of agrochemical spray deposition in vineyards at multiple phenological stages using 2D LiDAR-based primary canopy attributes

Anice Cheraiet, Olivier Naud, Mathilde Carra, Sébastien Codis, F. Lebeau, James Taylor

Predicting the site-specific distribution of agrochemical spray deposition in vineyards at multiple phenological stages using 2D LiDAR-based primary canopy attributes

A. Cheraiet[a,b,*], O. Naud[a], M. Carra[a], S. Codis[b], F. Lebeau[a,c] and J. Taylor[a].

[a] ITAP, Univ Montpellier, INRAE, Institut Agro, Montpellier, France

[b]IFV French Vine and Wine Institute, 3430 Route de l'Espiguette, Le Grau-du-Roi, France

[c]Biosystems Dynamics and Exchanges (BioDynE), TERRA Teaching and Research Center, Gembloux Agro-Bio Tech, University of Liege, Gembloux, Belgium

*Correspondence: anice.cheraiet@vignevin.com

Abstract

Predicting the dose to be applied on the basis of the structural characteristics of the plant canopy is a crucial step for the optimization of the spraying process. Mobile 2D LiDAR sensor data and local measurements of deposition rates from a face-to-face sprayer were made across eight fields in two Mediterranean vineyards at four dates in 2016 and 2017. Primary canopy attributes (height, width and density) were calculated from the LiDAR sensor data and the leaf wall area (LWA) determined. Multivariate models to predict the deposition distribution, as deciles, as a function of the primary canopy attributes were constructed and calibrated using the 2017 data and validated against the 2016 data. The prediction quality and uncertainty of these multivariate statistical models at various stages of growth was evaluated by comparison with a previously proposed univariate deposition models based on LWA at the same growth stages. The results showed that multivariate models can predict the distribution of deposits from a typical face-to-face sprayer more accurately ($0.76 < R^2 < 0.94$), and robustly ($10\% <$ nRMSEp $< 24\%$) than LWA-based univariate prediction models over the whole growing season. This improvement was especially clear for the lowest deciles (D1 to D5) of the deposition distribution. Results also demonstrated the importance of canopy density to provide relevant and complementary information to canopy dimensions when predicting deposition deciles with the multivariate models. The improved ability of multivariate models to predict underestimated deposition ($-1.5\% >$ bias $> -3.2\%$) when compared to univariate models makes it possible to consider a

reduction in the plant protection products while guaranteeing a safety margin for winegrowers when spraying. These predictive multivariate models could enable variable-rate sprayers to modulate doses at an intra-plot scale, which would allow a potential reduction in the quantities of plant protection products to be applied.

Keywords: Canopy density; Variable-rate spraying; 3D vine; Leaf Wall Area; Log-linear models

1. Introduction

The current regulatory context, and the very high societal demand for a reduction in the use of pesticides in viticulture, has led to a reconsideration of the entire plant protection process (EPPO, 2016). Achieving the objective of reducing pesticides will require the implementation of different and complementary approaches, including biological control (Flint and van den Bosch, 1982), the selection of resistant varieties (Vivier and Pretorius, 2002), optimization of spraying technologies (Llorens et al., 2011a) and adjustment of plant protection product (PPP) doses according to vegetation architecture (Walklate et al., 2011). Dose adjustment based on varying canopy size and shape, has been widely discussed in previous research (Gil et al., 2019), and seems especially important in countries, like France, where the registered dose rates of PPPs are still based on a fixed value per hectare (Codis, 2016) and calculated independently of the quantity of vegetation to be treated. There are two interrelated issues concerning dose reasoning. The first is dose expression. Some authors believe that a new dose expression that explicitly takes into account canopy development, which will be mostly influenced by growth stages, training systems and varietal characteristics, would be an important step toward a more efficient use of PPPs (Solanelles et al., 2006). The second issue is to define and select the most suitable crop parameters to be used for locally adjusting dose rates to canopy architecture (Walklate et al., 2011).

Historically, simple manual measurements of primary canopy attributes, such as height, width and the distance between rows, have been used to generate integrative indicators of canopy geometry, such as

58 the leaf wall area (LWA) (Koch, 1993) or tree row volume (TRV) (Byers et al., 1971). These
59 integrative indicators have become widely used as they provide a simple expression of the complex
60 architecture of the vegetation for modelling the PPP dose to be applied (Walklate and Cross, 2012). In
61 particular, the LWA has been identified as a good compromise between accuracy and simplicity to
62 establish a linear relationship between canopy geometry and the recommended amount of PPP
63 (Walklate and Cross, 2012) and it is now used to standardise PPP trials. However, the derivation of
64 these integrative indicators has two disadvantages: (i) they are too simplistic to properly model foliar
65 deposition (Cheraiet et al., 2019) under variable production conditions as the same LWA or TRV
66 value may reflect very different vegetation characteristics and PPP needs; and (ii) they are typically
67 based on measurements at only a few points within a vineyard with an assumption of a homogeneous
68 canopy structure over the entire area. When sampling is scarce, then local, site-specific variations in
69 canopy geometry cannot be taken into account when applying PPP.
70
71 To address the limitation in the spatial resolution of manual measurements, different high-resolution
72 spatial sensing systems have been proposed in recent years (Rosell and Sanz, 2012). Among these,
73 LiDAR systems have been reported to be effective for site-specific measurements of canopy size and
74 shape (Colaço et al., 2018). LiDAR sensors make it possible to obtain digitalised 3D point clouds,
75 from which a large amount of plant architecture information, such as canopy height, width (Rosell et
76 al., 2009;) and density (Walklate et al., 2002; Llorens et al., 2011b) can be obtained with a high level
77 of accuracy and repeatability (Moorthy et al., 2011). Due to the high spatial resolution of these LiDAR
78 data, these attributes can be calculated at any scale, from individual vines to entire vineyards.
79
80 Obtaining primary canopy dimensions from sensors, including LiDAR sensors, enables the calculation
81 of integrative indicators, such as the TRV or LWA, at high spatial resolutions. So far, this ability has
82 been used to build univariate empirical models to predict the mean foliar pesticide deposition (Llorens
83 et al., 2010), typically using power or logarithmic regression models (Siegfried et al., 2007; Bastianelli
84 et al., 2017). Bastianelli et al. (2017) highlighted the ability of these univariate empirical models to
85 discriminate between different types of spraying equipment and noted that the prediction quality for a

side-by-side sprayer using a univariate empirical based on LWA was sufficient to be considered for production applications.

However, empirical models that are based on a unique integrative indicator do have limitations, particularly when the objective is to adjust dose rates under a wide variety of vineyard conditions and training systems (Llorens et al., 2010). Vine management and pruning is normally standardised within blocks, which results in a strong correlation between canopy height and width. However, across different blocks, vineyards and regions, the relationship between primary canopy attributes differs according to local trellising systems, management strategies and vine varieties. Cheraiet et al. (2019) demonstrated that the prediction uncertainty of univariate empirical models varied greatly between vineyards in southern France, especially in the early stages of vegetation development when correct PPP is needed for effective crop protection. Moreover, univariate empirical models have only been used to predict the mean deposition, and not the distribution of deposition within the canopy. The distribution of deposition within the canopy will be dependent on both the characteristics of the canopy (Palleja and Landers, 2015) and the characteristics of the sprayer (type and settings: nozzle type, size and pressure, air velocity and airflow direction) (Derksen et al., 2007).

Therefore, whilst integrative indicators have proved useful for the industry when used with low-resolution measurements, their suitability for the development of precision spraying approaches using high-resolution information from sensing systems is questionable, especially when knowledge of deposition distribution rather than mean deposition is desirable. Sensor systems are now capable of generating high-resolution spatial and temporal information on primary canopy attributes, including height, width and some indication of density. However, so far, canopy density information has not been well incorporated into deposition prediction models within a vegetation canopy, even though the literature highlights the importance of this attribute (Pergher and Petris, 2008). It follows that multivariate statistical modelling approaches to predict the distribution of deposits at different stages of canopy development that are based on primary canopy attributes should be investigated, and are

hypothesised to be better than previously used univariate modelling approaches based on an integrative indicator of canopy architecture.

In order to test this hypothesis and to facilitate the optimization of spraying efficiency, the research presented here aims to investigate the use of multivariate statistical models to predict the distribution of deposits based on primary canopy attributes (dimensions, density) derived from a LiDAR sensing system. The specific objectives are to:

(1) Propose a primary canopy density attribute, based on 2D LiDAR data, that can be included in the modelling;

(2) Construct, calibrate and validate multivariate models, based on primary canopy attributes, to predict the distribution of intercepted deposits in vineyard canopies applied by a side-by-side sprayer at multiple growth stages over the growing season;

(3) Assess the prediction quality and uncertainty of these multivariate models relative to a previously proposed univariate model that is based on an integrated indicator of canopy size (LWA).

2. Materials and Methods

2.1. Fields trials

Two vine estates with blocks of different varieties and contrasting vigour were chosen for the study in 2016 and 2017. The 2016 trials were at the Mas Piquet Estate in Grabels, close to Montpellier, Hérault, France, and the 2017 trials at the Domaine Chapitre Estate in Villeneuve les Maguelone, Hérault, France. The training system, vine vigour and grape varieties in the two estates are characteristic of vineyards in southern France. Vines were trellised in 2.5m rows with a 1.0m vine spacing within rows using a cordon Royat or Guyot system that comprised a cordon wire and at least one trellising wire.

In 2016, spray deposition measurements and 2D LiDAR sensor canopy characterization was performed on four plots with four different varieties, while in 2017, measurements were performed on five plots with five different varieties. In both years there were 4 surveys (dates of measurements) that generated a range of growth stages (BBCH scale, Lorenz et al., 1994) due to phenological differences between varieties on a given date. These were: 3rd leaves unfolded (14), inflorescences clearly visible (53), inflorescences swelling and flowers closely pressed together (55), inflorescences fully developed and flowers separating (57), beginning of flowering: 10% of flowerhoods fallen (61), flowering (70), berries pea-sized and bunches hang (75), berry development (76), berries beginning to touch (77) and beginning of ripening (81). Full details of varieties, dates of measurements and growth stages are given in Table 1.

Table 1. Plot characteristics and phenological stages (BBCH scale) for each measurement dates 2016 and 2017 trials.

Block ID	Variety	Dates – 2016			
		T1: 03/05/2016	T2: 25/05/2016	T3: 23/06/2016	T4: 18/07/2016
Collection	*Marselan*	55	57	75	77
Faysse	*Chardonnay*	53	57	77	77
Franquet	*Cabernet Sauvignon*	14	55	75	77
Verdot	*Petit Verdot*	53	57	75	77
		Dates – 2017			
		T1: 28/04/2017	T2: 22/05/2017	T3: 14/06/2017	T4: 31/07/2017
Aranel	*Aranel*	57	62	75	81
Marselan	*Marselan*	57	61	75	81
Caladoc	*Caladoc*	57	61	75	81
PetitVerdot	*Petit Verdot*	57	62	75	77
Syrah	*Syrah*	57	61	75	85

2.2. Sprayer characteristics

An air-assisted side-by-side sprayer (Precijet, Tecnoma ®, Epernay, France) with nozzles set on vertical booms in front of each side of the canopy was used for all trials. Each boom was fitted with four hollow cone nozzles (TXA800067VK, Teejet, Wheaton, USA) aligned in a vertical plane to spray

157 the entire canopy. The Precijet is a more efficient sprayer than the pneumatic arch-type sprayers more
158 commonly used in the vineyards of southern France. For each spraying date and each block, sprayer
159 settings (number and direction of nozzles) were adapted according to the canopy size following good
160 agricultural practices and were not altered from one sampling site to another during block spraying. At
161 all dates and blocks, the working pressure was 0.5 MPa and the total flow rate was 5.5 L min^{-1}. At a
162 forward speed of 5 km h^{-1} the spray volume was 150 L ha^{-1}.
163
164 ***2.3. Data collection***
165
166 *2.3.1. Measurements of spray deposition*
167
168 For each date and each block, a 15 m section of a vineyard row was chosen under two constraints; i)
169 that it represented typical growth for the phenological stage and ii) that it was as homogeneous as
170 possible, i.e. sections with missing, over vigorous or under vigorous vines were avoided. Spray
171 deposition for each application was determined by including a chemical tracer in the spray application
172 and embedding part of the 15m section with artificial collectors. Different 15 m long sections were
173 chosen from one date to another to ensure that measurements were not affected by previous survey
174 activities.
175
176 The deposition sampling scheme differed slightly for the two years. In 2016, four consecutive vines
177 segments were sampled within each 15 m section. On each vine segment, 0.004 m^2 polyvinyl chloride
178 (PVC) collectors were positioned on the leaves inside the canopy in several planes according to a
179 profile perpendicular to the row according to a cell grid 0.2 m high and 0.1 m wide. In 2017, two
180 three-vine segments (that were termed a "trio") were sampled within each 15 m section. Within each
181 trio, a regular grid of the 0.004 m^2 PVC collectors was established in several planes; however, at a
182 lower density with a spacing of 0.4 m vertically and 0.1 m horizontally. Each trio in 2017 and each
183 four-vine section in 2016 will be called hereafter a "sampling unit". Details of the number of collectors
184 analysed for each sampling unit at each sampling date are given in Table 2.

185

Table 2. Number of collectors sampled (with spray deposits) in 2016 and 2017 for each sampling unit selected within the 15 m long plots. In 2016 there was one 4-vine section per 15 m and in 2017 there were two 3-vine sections sampled per 15 m of vine row.

Block ID	Sampling unit ID	Dates - 2016			
		T1: 03/05/2016	T2: 25/05/2016	T3: 23/06/2016	T4: 18/07/2016
Collection	A	28	95	109	117
Faysse	B	30	61	65	101
Franquet	C	30	52	95	121
Verdot	D	30	62	120	101
		Dates - 2017			
		T1: 28/04/2017	T2: 22/05/2017	T3: 14/06/2017	T4: 31/07/2017
Aranel	A1	34	37	71	66
	A2	29	51	69	72
Marselan	B1	24	46	68	66
	B2	27	50	66	67
Caladoc	C1	32	47	67	69
	C2	28	48	65	59
PetitVerdot	D1	22	38	48	47
	D2	22	36	53	47
Syrah	E1	21	NA[†]	67	67
	E2	25	NA[†]	64	69

186 [†] No deposition data on the Syrah block on 22/05/2017 following a problem of accessibility to the
187 block due to phytosanitary treatments.
188
189 A quantitative assessment of the spray distribution in the canopy was made by measuring the
190 deposition of a colorimetric tracer, Tartrazine E-102 (Sigma, St. Louis, MO, USA) on the PVC
191 collectors (Codis et al., 2018). For each spray campaign, the sprayer was filled halfway with distilled
192 water and the necessary amount of Tartrazine was added to achieve a target concentration of 10 g. L^{-1}.
193 This solution was then sprayed, reproducing normal spraying procedures. After the tracer had
194 completely dried, all PVC collectors were retrieved and placed in individual bags. In the laboratory,
195 each individual PVC collector was rinsed in a known volume of distilled water to recover the
196 Tartrazine and the concentration was measured with a spectrophotometer at 427 nm (Uviline 9100,
197 resolution: 0.001, accuracy ± 0.003, Secomam, Champigny sur Marne, France). Deposition was
198 normalised according to the collector surface and to the Tartrazine dose rate ha^{-1}. Spray deposits were

199 expressed in nanograms per square decimetric of leaves for 1 g sprayed ha^{-1} (ng dm^2 per 1g ha^{-1})
200 (Codis et al., 2018).
201 It should be noted that many physical effects influence deposition values, including variation in the
202 spray trajectory angle, anisotropic leaf area distribution, streamlining of leaves in the air flow and
203 small-scale aerodynamics of spray droplets (Walklate et al., 2011). These effects are either considered
204 constant or impractical to measure. The sampling design, based on a regular 2D grid across the canopy
205 row along a minimum length of 3 m of vine row, was designed to minimise any of these potential
206 effects.
207
208 Artificial collectors are often used as replacements for natural foliage in research studies as the
209 recovery of sprayed tracer retained on natural plant surfaces is more difficult and more expensive than
210 from artificial targets. Furthermore, research using natural targets is always limited by the size and
211 spatial heterogeneity of the sample, and these parameters play an important role in the unbiased
212 estimation of deposition in vegetation (Forster et al., 2014). PVC collectors have been demonstrated to
213 have a good recovery rate and are efficient in recovering the spray deposits (Garcerá et al., 2012).
214 From the results presented in the literature, this study used the hypothesis that the distribution of
215 deposits intercepted on PVC collectors is near to the distribution actually observed on vine leaves.
216
217 Historically, deposits onto vine leaves or PVC collectors (Codis et al., 2018), have been aggregated to
218 give a mean deposition per sampling unit, without taking into account the variability or spatial
219 distribution of deposition rates within the sampling unit. However, in order to ensure optimal crop
220 protection, it is assumed here that the attribute space can be characterised more precisely by a
221 statistical distribution rather than a mean. Using the statistical distribution, rather than a mean of
222 deposition, makes it possible to account for the variability of locally intercepted deposits and to avoid
223 PPP under-dosing, regardless of the area in the canopy where this under-dosing may occur.
224
225 As the intent here is to examine if and how spray deposition varies within the canopy, the distribution
226 of deposits across all vineyards for each individual survey (date) were aggregated and described using

227 deciles. It is worth noting that although the PVC collectors were located in a regular 2D grid across the
228 canopy, their physical location has not been explicitly used in the modelling. The crop management
229 hypothesis is that if the attribute space can be modelled more accurately with a statistical distribution
230 rather than a mean, then management can be altered to avoid under-dosing, regardless of where it
231 occurs in the canopy.
232
233 *2.3.2. 2D LiDAR information of canopy structure*
234
235 A Sick LMS100 (SICK AG, Düsseldorf, Germany) 2D LiDAR sensor was used in the study. The
236 LMS100 is a fully-automatic divergent laser scanner based on time-of-flight (TOF) measurement with
237 a typical error of ± 30mm, a selectable angular resolution ($\Delta\theta$) set to 0.5° and a range of 270°. With
238 these settings, there were 541 distances recorded for one complete laser rotation, which is hereafter
239 referred to as a "scan", and scans were obtained at 50 Hz. The LMS100 and data logging system were
240 mounted on a purposely-built stainless-steel mast fixed behind the tractor operating the sprayer,
241 according to a previously described procedure (Cheraiet et al., 2020). The LMS100 sensor height
242 ranged from 1.0 – 1.4m above ground level and was adjusted up during the season to account for
243 increasing canopy height. The tractor was driven along the vineyard rows at a constant forward travel
244 speed of 5 km h^{-1}, with a typical error of ± 0.21 km h^{-1} (IFV, internal report, October, 2018).
245
246 This sensing system was coupled to a Real Time Kinematic (RTK) GNSS receiver (Teria GSM
247 correction, Vitry-sur-Seine, France) to identify the start and end point of the sampling units. Once the
248 starting point was set, scans were aggregated using a fixed forward distance based on the constant
249 tractor speed to generate a 3D point cloud reconstruction of the vine environment. The sprayer
250 replicated commercial operations, i.e. the tractor only traversed every second row so that the canopy
251 was only scanned from one side. This differs to most previous research activities with LiDAR sensors,
252 but was deliberately done to approximate commercial conditions. Full details of the system set-up are
253 given in Cheraiet et al. (2020).
254

255 *2.3.2.1. Derivation of primary canopy attributes*

256

257 The determination of primary canopy dimensions (height and width) from the filtered LiDAR data was
258 performed using the LiDAR bayesian point cloud classification algorithm (BPCC) (Cheraiet et al.,
259 2020). This is achieved by (a) a 1D cluster analysis of the LiDAR point clouds to identify different
260 components of the vine and trellis system (trunk, vegetation zone, trellis wire), followed by a Bayesian
261 classification, and (b) an estimation of canopy height and width using an adjustable statistical
262 threshold to improve canopy dimension estimates as the canopy develops. For canopy width, the
263 method derives a half-vine width, as only one side of the canopy is scanned, and assumes symmetry to
264 derive the full vine canopy width. Full details of the BPCC method are in Cheraiet et al. (2020).

265

266 Several indicators for vegetation density based on 2D LiDAR acquisition have previously been
267 proposed but have drawbacks for use in predicting deposition distributions in the canopy. The density
268 metric proposed by Llorens et al. (2011b) exhibits a strong collinearity with vegetation height and is
269 discrete in nature (5 classes), making it less suitable for modelling. The tree area index (TAI) proposed
270 by Walklate et al. (2002) has been shown to be sensitive to the length of the vine row section scanned
271 and is only recommended for > 1 m row sections (Arnó et al., 2013). This limits its usefulness for
272 multi-scale dose modulation methods, especially if real-time and high resolution dose modulation are
273 to be considered. Therefore, an adapted estimation of canopy density using LiDAR data, called the
274 intercepted beam rate (IBR), is proposed here. The IBR is similar to the metric of Llorens et al.
275 (2011b) except that it is restricted to interceptions in the canopy zone defined by the BPCC algorithm.
276 It is expressed as a continuous value, not a class, generating more degrees of freedom to characterise
277 heterogeneity in the canopy density. The IBR (%) is defined as (Eq. 3):

278

279 $$\mathrm{IBR} = \frac{\mathrm{NBI}}{\mathrm{NBE}} * 100 \qquad \text{Eq. 3}$$

Where: NBI is the number of beams intercepted between angles that define the range of the canopy zone height along a trellis and NBE is the total number of beams emitted over the same angular range. The mean IBR was calculated for each sampling unit.

2.3.2.2. Integrated indicator: Leaf Wall Area

The LWA is the area of leaf based on the assumption that the canopy sides are completely flat, and hence, form a "wall". The LWA has been chosen at the European Union level as the new metric to support dose expression in 3D cropping systems when performing efficacy trials during registration processes (EPPO, 2016). The LWA is expressed in square metres per hectare (m^2 ha^{-1}) and defined as (Eq. 4):

$$LWA = \frac{2 \times VH \times 10{,}000}{RS} \quad \text{Eq. 4}$$

Where: VH is canopy height (m); 10,000 is the ground area (m^2) and RS is the row spacing (m).

The LWA is derived from canopy height and row spacing only, with the later usually a constant in vineyards. Therefore, while LWA is considered an integrative metric, it is directly correlated to canopy height. Canopy width and density information is not included.

2.4. Modelling

Previous approaches to modelling intercepted spray deposits within a crop canopy have used power (Bastianelli et al., 2017) or logarithmic (Siegfried et al., 2007) laws to model mean depositions. As the intent here is model deposition distribution, not mean deposition, log-lin regression models were used to improve model behaviour and fitting at the upper and lower limits of the distribution.

306 The data acquired on the 2017 and 2016 plots were used as calibration and validation sets respectively.
307 The 2017 data was used for calibration as it had a higher number of PVC collectors per sampling unit
308 (Table 2) and the 2017 survey encompassed a longer phenological period (Table 2). The calibration
309 data were used to develop both univariate and multivariate regression models for predicting foliar
310 deposits distributions, while the validation data were used to evaluate the performance of the
311 developed models.
312
313 Univariate empirical models for the prediction of foliar deposit distributions were derived using the
314 integrative indicator (LWA) as the sole predictor. This formed a "standard" model based on the
315 current European standard. For each decile of the deposition distribution, a log-lin regression model
316 was used (Eq. 5).
317
318 $$y_{i,j} = U_j e^{-(\eta_j * LWA_i)} + e_{i,j}, \quad y_{i,j} > 0 \qquad \text{Eq. 5}$$
319 Where: $y_{i,j}$ represents the value of the j[th] decile of spray deposit in the i[th] vine trio with $\forall i \in [1, 40]$
320 and $\forall j \in [1,9]$, e_i are random variables, it is assumed that e_i are independent and $\varepsilon_i \sim N(0, \sigma^2)$, LWA_i
321 is the leaf wall area for the sample site in the i[th] sampling unit, U_j and η_j are real unknown parameters
322 that will have to be estimated, where U_j is the intercept and η_j is the slope of the model equation for
323 the prediction of j[th] decile.
324
325 Multivariate models for prediction of decile deposition as a linear combination of primary canopy
326 attributes (VH, VW and IBR) were similarly constructed using the same log-lin model form (Eq. 6).
327
328 $$y_{i,j} = M_j e^{-(\alpha_j * VH_i + \beta_j * \mathrm{VW}_i + \gamma_j * \mathrm{IBR}_i)} + e_{i,j}, \quad y_{i,j} > 0 \qquad \text{Eq. 6}$$
329 Where: $y_{i,j}$ represents the value of the j[th] decile of spray deposit present in the i[th] vine trio with $\forall i \in$
330 $[1, 40]$ and $\forall j \in [1,9]$, e_i are random variables, it is assumed that e_i are independent and
331 $\varepsilon_i \sim N(0, \sigma^2)$, VH_i is the mean value of vegetation height measured at the i[th] vine trio, VW_i is the mean
332 value of vegetation width measured at the i[th] vine trio, IBR_i is the mean value of intercepted beam rate

measured at the i[th] vine trio, M_j, α_j, β_j and γ_j are real unknown parameters to be estimated, where M_j is the intercept and $\alpha_j, \beta_j, \gamma_j$ are the slopes corresponding respectively to VH, VW and IBR in the model equation for the prediction of j[th] decile.

A stepwise forward approach was used to identify the most parsimonious prediction model (uni-, bi- or tri-variate) as well as the statistical weight of each predictor in the models. Models for each deposition decile were ranked using the corrected Akaike's Information Criterion (AICc) as the number of data were limited (≤ 40 data points) (Hurvich and Tsai, 2001).

Multicollinearity among the explanatory variables was tested using the variance inflation factor (VIF) (Akinwande et al., 2015) (Eq. 7): The VIF was calculated for each multivariate model used to predict a decile deposition and VIF > 5 set as a threshold to indicate relatively high levels of multicollinearity in the models.

$$VIF = \frac{1}{1-R^2} \quad \text{Eq. 7}$$

Where: R^2 is the coefficient of determination of the prediction model.

2.5. Model Evaluation

The coefficient of determination (R^2) and the normalised root mean square error (nRMSE) were used to evaluate the fit of the calibration models (2017 data). The nRMSE was used to facilitate comparison between models of all the deposition deciles and is defined as a percentage (Eq. 8):

$$nRMSE_j = \frac{\sqrt{\sum_{i=1}^{N} \frac{(\hat{y}_{i,j} - y_{i,j})}{N}}}{\bar{y}_{i,j}} * 100 \quad \text{Eq. 8}$$

Where: $\hat{y}_{i,j}$ are estimated values for the j[th] decile, $y_{i,j}$ are observed values for the j[th] decile and $\bar{y}_{i,j}$ are the mean of observed values for the j[th] decile, and N is the number of observations.

The performance of the univariate and multivariate decile models, when applied to the validation data, was assessed by analysing the observed vs. predicted values by the (i) R^2 of a 1:1 linear regression fit, (ii) model bias (%) and, (iii) normalised root mean square error of prediction (nRMSEp) (normalised by the mean of the predicted decile deposit values). Again the nRMSEp is defined as a percentage (Eq. 9):

$$nRMSEp_j = \frac{\sqrt{\sum_{i=1}^{N} \frac{(Y_{i,j} - y_{i,j})}{N}}}{Y_{i,j}} * 100 \quad \text{Eq. 9}$$

Where: $Y_{i,j}$ are predicted values for the jth decile, $y_{i,j}$ are observed values for the jth decile and $\bar{y}_{i,j}$ are the mean of predicted values for the jth decile, and N is the number of observations.

All analyses were performed using the open source statistical R Software® (Version 1.2.5001) (R Development Core Team, 2020). Respectively, for the AIC, nRMSE and VIF calculations, the stats4 (version 3.6.2), Metrics (version 0.1.4), car (version 3.0.10) packages were used.

3. Results and discussions

3.1. Data description

3.1.1. Description of the deposition data

The deposition distributions exhibited a positive skewness, associated with very high deposition rates on the external canopy PVC collectors. The 10th decile skewed the distribution and was characterised by oversaturation relative to the target dose. It is commonly accepted by growers and experts that the external canopy layers that face the sprayer will exhibit this phenomenon to achieve adequate deposition in the internal layers. As oversaturation is assumed to ensure protection, the 10th decile was excluded from subsequent analyses and only the first nine deciles were used for modelling.

387 The empirical density curve of the depositions recorded by the PVC collectors positioned within the
388 vine trios in 2017 showed a clear trend towards a decrease in mean deposition associated with
389 increasing vine growth over time that is being sprayed with a constant quantity of tracer (Fig. 1). The
390 deposition distributions followed a Poisson-type form and the shape of the distribution changes over
391 time, with the mean and the variance decreasing as the season progresses. The median foliar
392 deposition ranged from 500 ng dm² per 1g ha^{-1} in T1 to 195 ng dm² per 1g ha^{-1} in T4.
393
394 Figure 1 near here
395
396 The Poisson distributions indicated that a unique and central statistic (mean or median) of the deposit
397 was insufficient to describe the data, even if completed by a quantification of variance. This highlights
398 the problem of modelling deposition using the mean and supports the use of the decile by decile
399 analysis in order to take into account the statistical dispersion of deposition values.
400
401 Deposition rates also varied between varieties at a given date, with inter-block variability being
402 greatest early in the season (at T1, 38%) and lowest at the latest observation (T4, 11%) (data not
403 shown). This can be explained by differences in the timing of bud-burst and shoot development
404 between the grape varieties early in the season (Table 1). Even at full canopy development (T3-T4),
405 some differences in shoot length, leaf size and shape and vine morphology between varieties still
406 existed, despite the common trellising systems between vineyards.
407
408 *3.1.2. LiDAR-derived canopy data*
409
410 Summary plots of the primary canopy attributes (VH, VW and IBR) derived from the LiDAR sensor
411 survey in the 2017 survey blocks, at a resolution scale of 3 m (same as vine trio scale used for
412 sampling deposits) are shown in Figure 2.
413
414 Figure 2 near here

Table 3. Summary of canopy height (VH) and width (VW) and density (IBR) data obtained at the four LiDAR acquisition dates in 2017.

	T1	T2	T3	T4
Vegetative parameters		Mean		
VH (m)	0.65	0.99	1.24	1.19
VW (m)	0.38	0.59	0.83	0.81
IBR (%)	28.2	45.3	59.1	72.4
		CV (%)		
VH	13.1	14.5	16.2	17.1
VW	10.2	16.6	11.5	5.3
IBR	9.4	12.7	12.3	19.6

Vegetation height and width (Figs. 2a-b) increased almost linearly from bud break (T1) to green pea stage (T3), which is approximately the date of the first canopy trimming operation. Trimming, combined with increasing water stress over summer, tends to stagnate any further growth. This is reflected in a plateauing of VH and VW between T3 and T4 (Table 3), which indicated that these parameters were likely to be less informative about changes in canopy conditions towards the end of the season. Overall, the earlier varieties (Aranel, Marselan and Caladoc) had larger dimensions than the later developing variety (Petit Verdot) that never caught up in size to the other varieties (Figs. 2a-b). On average, over the survey period (T1-T4), the inter-block variability was 15.2% and 11% for VH and VW respectively. This showed that there were real differences between blocks during the growing season (Table 3).

In contrast to VH and VW, the IBR canopy density metric (IBR) did not plateau in any block between T3 and T4, despite the in-season canopy trimming operations (Fig. 2c). This indicated that IBR could provide relevant information to characterise the canopy later in the season. The variability of the IBR metric also increased as the season progressed, with the IBR parameter having a CV of 9.4% in T1, 12.7% in T2, 12.3% in T3 and 19.6% in T4 (Table 3). This higher variability of the mid- to late-season IBR corresponds to the period when mean deposits were lowest (Fig. 1).

3.2. Modelling

3.2.1. Univariate models

The results of the univariate model construction for deciles 1-9 (D1-D9) with the calibration data set showed a relatively stable relationship ($0.69 < R^2 < 0.82$) for the prediction of foliar deposition using the LiDAR-derived LWA indicator (Table 4). The first two deciles (D1-D2) had the lowest prediction quality (R^2) and the greatest error of the prediction models (nRMSE) (Table 4). The mean deposition was also modelled, which is the current recommended approach, and explained 80% of the variance in the mean deposition in the canopy.

Table 4. Parameters and quality indicators of univariate models for prediction of decile deposition over the entire growing season: indicating model coefficients (U and λ) and quality indicators for each decile model for both the calibration (R^2 and nRMSE) and validation (R^2 of 1:1, nRMSE and bias) stages. The equivalent mean model (current standard reference) parameters and quality indicators are also shown.

Deciles distribution deposit	Model equation		Calibration (2017) (n=40)		Validation (2016) (n=16)		
	U	λ	R^2	nRMSE (%)	R^2 of 1:1 line	nRMSEp (%)	Bias (%)
D_1	740.6	2.35E-04	0.69	46	0.66	45	-5.8
D_2	935.39	2.54E-04	0.75	36	0.77	41	-4.8
D_3	1282.13	2.61E-04	0.79	28	0.80	37	-3.9
D_4	1524.34	2.58E-04	0.81	25	0.75	34	-2.3
D_5	1702.88	2.47E-04	0.81	19	0.80	30	2
D_6	1820.63	2.35E-04	0.78	17	0.82	27	2.9
D_7	2100.3	2.30E-04	0.80	18	0.83	25	2.1
D_8	2474.84	2.25E-04	0.79	20	0.85	29	7.6
D_9	3045.88	2.19E-04	0.82	21	0.81	34	8.4
mean	1789.88	2.40E-04	0.80	18	0.79	26	2.2

Applying the calibrated model to the independent validation data (2016) generated prediction accuracies for the univariate decile models that were similar to and followed the same trend as the calibration models ($0.66 < R^2 < 0.85$), with lower deciles being associated with lower prediction

452 quality (Table 4). The bias values were negative for the validation models predicting deciles D1 to D4
453 and positive for deciles D5 to D9 (Table 4). The lower deciles represent areas of the canopy where a
454 below mean level of deposition was achieved, which may be insufficient for effective crop protection.
455 In these deciles, the univariate model underestimated (negative bias) depositions in the already poorly
456 covered (low deposition) areas.
457
458
459 Figure 3 near here
460
461 The model fit for the median deposition (D5) is shown as an example (Fig. 3). The overestimation at
462 higher deposition rates, associated with T1 (red squares; early season), is evident. Correct application
463 of early season PPPs is important for prophylactic protection of the plant and a systematic
464 overestimation of deposition is undesirable. However, when the canopy is small (early season), the
465 median depositions were very high (Fig. 1), so with a fixed dosage per hectare there is little risk of
466 under-application. This may change if dose expression regulations are altered in the future to minimise
467 the risk of early season over-applications and to improve the use-efficiency of PPPs. For T2, T3 and
468 T4, the median deposition from the model underestimated real conditions, i.e. it was likely that there
469 was more being applied than was being modelled. However, under the fixed dose expression
470 regulations, the amount of deposition per canopy surface area was dropping as the canopy increased,
471 so under-applications are more likely. Underestimation is preferable to overestimation under these
472 conditions, although correct estimation is preferred. The ability of the univariate model to robustly
473 predict median foliar deposition throughout the growing season was not assured. This can be
474 explained by the fact that the univariate approach only accounted for VH in the LWA, but not VW or
475 canopy density.
476
477 *3.2.2. Multivariate models*
478

479 The VIF analysis indicated that there was no multicollinearity (VIF < 5) between the primary canopy
480 attributes (VH, VW and IBR) in the multivariate decile deposition models. The stepwise parameter
481 selection showed that the IBR metric had the strongest contribution to the D1-D3 models, followed by
482 VW and then VH. Thus for low deposition values, which are more common at the end of the growing
483 season (T3 and T4), the IBR was dominant for predicting deposition (Table 5). For the D7-D8
484 prediction models, which corresponded to high deposition values, VH and VW were the strongest
485 predictors, followed by IBR (Table 5). Therefore, when the canopy was developing (T1 and T2)
486 information on VH and VW was important for modelling deposition. Once the canopy had reached
487 full size (T3 and T4) and VH and VW had stabilised, the importance of VH and VW diminished.
488

Table 5. Multivariate models for predicting of decile deposition: comparison of the relative weight (order of occurrence in the model (1, 2 or 3)) of the primary canopy attributes (VH, VW and IBR) according to the conditional Akaike information criterion and study of the multi-collinearity between the primary canopy attributes by variance inflation factor (VIF).

Deciles model	Primary canopy attributes					
	vegetation height (VH)		vegetation width (VW)		Intercepted beam ratio (IBR)	
	order of occurrence in the model	VIF	order of occurrence in the model	VIF	order of occurrence in the model	VIF
1	3	1.63	2	1.59	1	2.09
2	3	2.13	2	2.34	1	2.02
3	3	1.81	2	2.98	1	2.67
4	2	3.22	1	3.74	3	3.06
5	2	3.32	1	3.45	3	2.06
6	2	3.35	1	3.75	3	1.61
7	1	2.78	2	2.1	3	1.94
8	1	2.37	2	3.36	3	1.62
9	1	3.53	2	3.74	3	2.53

489
490 The parameters for the fitted multivariate calibration models and model statistics for both the
491 calibration and validation models are shown in Table 6. Prediction quality was very good for both the
492 calibration ($0.81 < R^2 > 0.93$) and validation ($0.79 < R^2 > 0.94$) data sets and these followed the same
493 trend as the univariate approach, with lower fits at lower deciles. The nRMSE ranged from 22% to 7%

for calibration and 24% to 10% for validation (Table 6). The validation bias was negative for all nine prediction models (Table 6), indicating that the multivariate deposition decile models underestimated deposition for all deciles in the distribution. While underestimation was not desirable, a "worst-case" risk management modelling approach should encourage underestimation rather than overestimation of deposition, in order to ensure that PPPs are applied in sufficient quantity. Figure 4a shows the relationship between the observed and predicted median (D5) deposition for the multivariate case (comparable to the univariate case in Fig. 3). The data plots close to the 1:1 line, over the entire period of the study (T1 – T4), but consistently slightly underestimates depositions (Fig. 4a). The ability of the multivariate model to reliably predict median foliar deposition throughout the growing season was explained by its ability to account for the differential contribution of VH, VW and IBR to deposition as the canopy develops. The actual log-lin regression for the median deposition prediction model (D5), using the model parameters in Table 6, is shown in Figure 4b as an example.

Table 6. Parameters and quality indicators of multivariate models for prediction of decile deposition over the entire growing season: including model coefficients (M and α, β, γ) and quality indicators for each decile model for both the calibration (R^2 and nRMSE) and validation (R^2 1:1, nRMSE and bias) stages (same as Table 4). Decile 10 is not shown.

Deciles distribution deposit	Model equation				Calibration (2017) (n=40)		Validation (2016) (n=16)		
	M	α	β	γ	R^2	nRMSE (%)	R^2 of 1 :1 line	nRMSEp (%)	Bias (%)
D_1	847.32	1.06	0.3	1.28	0.81	22	0.79	24	-1.5
D_2	1057.31	0.97	0.48	1.13	0.83	20	0.81	21	-2.1
D_3	1506.97	0.82	0.37	1.54	0.88	10	0.83	15	-2.2
D_4	1819.9	0.7	0.36	1.69	0.92	9	0.87	12	-2.5
D_5	2055.62	0.55	0.34	1.81	0.93	9	0.94	13	-2.1
D_6	2154.46	0.52	0.47	1.59	0.88	7	0.91	10	-2.6
D_7	2530.31	0.38	0.43	1.77	0.91	8	0.9	12	-3.1
D_8	2976.56	0.34	0.46	1.75	0.9	10	0.9	13	-2.8
D_9	3578.82	0.39	0.55	1.5	0.91	11	0.89	14	-3.2

Figure 4 near here

3.3. Assessment of the performance of multivariate models compared to univariate models

For all decile levels, the multivariate model outperformed the univariate model (higher R^2, lower nRMSE) (Tables 4 and 6). The improved performance of the multivariate models was attributed to the additional information on canopy width and density available to the model, both of which influence deposition. The bias of the multivariate models was always negative (Table 6), unlike the univariate prediction models of deciles D5 to D9 that had a positive bias (Table 4). The overestimation of deposition at the early stages of the growing season, when the risk of pathogen occurrence and development is highest, is not problematic under current fixed dose regulations, as the real deposition rates are very high (Fig. 1). For systems where the dose expression is adjusted to expected canopy size, overestimation may be an issue and the use of the LWA to determine the dose to be applied presents a potential risk of underdosing (Rüegg et al., 2001). This would have potential consequences on the efficacy of PPP. These models need to be tested under these conditions, but the results here indicated that the multivariate model provided a more risk-adverse model for managing plant protection risk throughout all stages of the growing season. Thus, multivariate statistical models offer the possibility to react to the evolution and variability of vegetation during the season, so that it is possible to consider reducing the use of PPPs while providing a margin of safety to growers in terms of crop protection.

The low deposition values that constituted (D1-D4) were found at all four dates (T1 to T4) (Fig. 1). Therefore, the prediction models for D1-D4 take into account deposition data from all dates (T1 to T4), which may lead to these prediction models having poorer quality with regards to accuracy and uncertainty. In contrast, higher deposition values (greater than 500 ng dm^2 per 1g ha^{-1}) were only found at T1 and T2.

3.4. Potential uses of multivariate deposit prediction models

The current use of a fixed dose expression under European guidelines, which is independent of canopy size, is problematic. Guidelines are evolving and a first step toward this was the introduction of the LWA metric into calculations of dose expression in all situations (EPPO, 2016). However, this new LWA-based dose expression is based on the unproven hypotheses that (i) dose requirements are a function of a single integrative indicator and (ii) there is a strictly linear relationship between intercepted deposits and the quantity of vegetation canopy to be protected. The results from this study indicated that this relationship was not necessarily linear and that using individual canopy attributes in a multivariate model, rather than an aggregated canopy metric, provided more flexibility in the modelling process. As vine canopies evolve, the relative importance of different canopy dimensions for modelling depositions also changed. This flexibility and improve modelling will become more important if dose expression shifts from an analysis of mean deposition rates to an analysis of the expected distribution of deposition rates within a canopy. From the perspective of commercial applications, this is unlikely to become the norm in the near future; however, from a regulatory perspective and for testing and grading the performance of new commercial sprayers, the ability to better model the distribution of depositions will be very useful in promoting more effective and efficient spray systems.

Ultimately the ability of these, or similar, multivariate models will make it possible to consider a step change in the spray management paradigm from managing a mean deposition (Walklate et al., 2011) to managing the deposition distribution at any given time over the season. This will allow deposition in areas of the canopy that are least well treated (D1-D2) during a spray operation to be taken into account. The decomposition of the overall deposition into a distribution will be critical to a better epidemiological understanding of resistance and pathogen pressure after phytosanitary treatments have been carried out. In this study, the distribution has only been described in the attribute space, and not in the geographical (canopy) space. It is expected that the areas of lower deposition will be located in denser areas of the canopy with greater numbers of leaf layers between the target point and the sprayer; however, more research is certainly needed to develop approaches to spatialise the distribution of deposits within the canopy.

Furthermore, in view of the quality of the prediction models developed in this study at a trio scale (3m of trellised vineyard row), the application of these multivariate prediction models at such a small spatial scale offers interesting possibilities for the optimization of spraying in viticulture. If high-resolution spatial canopy dimensions, including density, are generated, then differential or variable-rate spraying could be performed in real-time. This can be achieved by sensing pre-spraying to develop prescription spray maps, or by sensing directly in front of a sprayer to perform real-time dose modulation (Llorens et al., 2010). The proposed modelling approach here, when tuned to sprayer characterisers, could be used to model and optimise deposition coverage whilst minimising the quantity of PPP applied. This is a clear objective for the industry (EPPO, 2016) and is not just dependent on good sensing and variable-rate technology but also on good decision support systems that require accurate predictive modelling capabilities. In addition to supporting differential spraying, improved deposition models could be applied site-specifically post-application to identify areas where the PPP application may have been sub-optimal i.e. where there is a disagreement between the amount applied and the amount modelled.

4. Conclusions

Optimization of the use of crop protection inputs in viticulture should take into account the structural characteristics of the vegetation. In this study, a multivariate statistical modelling approach was proposed to predict the mean and distribution of spray depositions as a function of primary vine canopy attributes (height, width and density) that were derived from a LiDAR sensor system. Results obtained from data collected over two years, on seven grape varieties and on two trellising systems, showed that the proposed multivariate statistical models can predict the distribution of depositions of a typical face-to-face sprayer more accurately and robustly than univariate prediction models based on a calculation of leaf wall area, the current industry standard. This ability to predict deposition distributions will allow areas of the vine canopy that are poorly treated (unprotected) after spraying to be taken into account and will provide a better understanding, from an epidemiological point of view,

of resistance and pathogen pressures in vineyards. In addition, the results provided clear indications of the ability of multivariate statistical models to react to changing canopy attributes over the season and spatially in the vineyard, such that it is possible to envisage using these models for a site-specific reduction in the PPP expected by the wine industry while guaranteeing a safety margin for growers when spraying.

Acknowledgments

The authors are indebted to the numerous individuals associated with IFV and UMR ITAP who have helped collect vineyard data: Y. Hudebine, X. Riberolles, E. Trinquier, X. Delpuech, A. Rico, P. de Jesus, A. Verges, A. Lienard, A. Kazakos, A. Mariette, V. de Runicki, M. Bastianelli, M. Lewis and E. Merlier. We also want to thank the staff members of the vine estates Domaine Mas Piquet and Domaine Chapitre for making their vineyard blocks available for our measurements. This work was supported by the French National Research Agency under the Investments for the Future Program, referred to as ANR-16-CONV-0004. Anice Cheraiet's PhD is cofunded by #DigitAg and Institut français de la vigne et du vin.

References

Akinwande, M. O., Dikko, H. G., Samson, A. (2015). Variance inflation factor: as a condition for the inclusion of suppressor variable (s) in regression analysis. Open Journal of Statistics, 5(07), 754. https://doi.org/10.4236/ojs.2015.57075

Arnó, J., Escolà, A., Vallès, J. M., Llorens, J., Sanz, R., Masip, J., Palacín, J., Rosell-Polo, J. R., 2013. Leaf area index estimation in vineyards using a ground-based LiDAR scanner. Precision Agriculture, 14(3), 290-306. https://doi.org/10.1007/s11119-012-9295-0

Bastianelli, M., Rudnicki, V. D., Codis, S., Ribeyrolles, X., Naud, O., 2017. Two vegetation indicators from 2D ground Lidar scanner compared for predicting spraying deposits on grapevine. Proceedings of the 2017 EFITA WCCA conference, Montpellier, France, 153-154.

621 Byers, R. E., Hickey, K. D., Hill, C. H., 1971. Base gallonage per acre. Virginia Fruit, 60(8), 19-23.
622 https://doi.org/10.1590/S0103-90162013000600003
623 Cheraiet, A., Carra, M., Lienard, A., Codis, S., Vergès, A., Delpuech, X., Naud, O., 2019.
624 Investigation on LiDAR-based indicators for predicting agrochemical deposition within a vine
625 field. In 12th European Conference on Precision Agriculture, Precision Agriculture '19 (July),
626 (Eds). J.V. Stafford, Wageningen Academic Publishers, 157-164. https://doi.org/10.3920/978-90-
627 8686-888-9_18
628 Cheraiet, A., Naud, O., Carra, M., Codis, S., Lebeau F., Taylor J. A., 2020. An algorithm to automate
629 the filtering and classifying of 2D LiDAR data for site-specific estimations of canopy height and
630 width in vineyards. Biosystems Engineering, 200, 450-465.
631 https://doi.org/10.1016/j.biosystemseng.2020.10.016
632 Codis, S., 2016. Stakes for a new model of dose expression in viticulture: advantages and points to be
633 taken into consideration. In Proceedings of the EPPO Workshop on harmonized dose expression
634 for the zonal evaluation of plant protection products in high growing crops, Austrian Agency for
635 Health and Food Safety Vienna,12-13.
636 Codis, S., Carra, M., Delpuech, X., Montegano, P., Nicot, H., Ruelle, B., Ribeyrolles, X., Savajols, B.,
637 Vergès, A., Naud, O., 2018. Dataset of spray deposit distribution in vine canopy for two contrasted
638 performance sprayers during a vegetative cycle associated with crop indicators (LWA and TRV).
639 Data Brief, 18, 415–421. https://doi.org/10.1016/j.dib.2018.02.012
640 Colaço, A.F., Molin, J.P., Rosell-Polo, J.R., Escolà, A., 2018. Application of light detection and
641 ranging and ultrasonic sensors to high-throughput phenotyping and precision horticulture: Current
642 status and challenges. Horticultural Research 5, 35. https://doi.org/10.1038/s41438-018-0043-0
643 Derksen, R. C., Zhu, H., Fox, R. D., Brazee, R. D., Krause, C. R., 2007. Coverage and drift produced
644 by air induction and conventional hydraulic nozzles used for orchard applications. Transactions of
645 the ASABE, 50(5), 1493-1501. https://doi.org/10.13031/2013.23941
646 EPPO (European Plant Protection Organization)., 2016. Conclusions and recommendations.
647 Workshop on harmonized dose expression for the zonal evaluation of plant protection products in
648 high growing crops. Vienne, 18–20 October 2016. Available online :

https://www.eppo.int/media/uploaded_images/MEETINGS/Conferences_2016/dose_expression/Conclusions_and recommendations.pdf (accessed on 11 November 2020).

Flint ML, van den Bosch R (1981) A history of pest control. In: Flint ML, van den Bosch R (eds) Introduction to integrated pest management. Springer, Boston, 51–81. https://doi.org/10.1007/978-1-4615-9212-9_4

Forster, W. A., Gaskin, R. E., Strand, T. M., Manktelow, D. W. L., Van Leeuwen, R. M. (2014). Effect of target wettability on spray droplet adhesion, retention, spreading and coverage: artificial collectors versus plant surfaces. NZ Plant Protection, 67, 284-291.

Garcerá, C., Moltó, E., Zarzo, M., Chueca, P. (2012). Modelling the spray deposition and efficacy of two mineral oil-based products for the control of Aonidiella aurantii (Maskell). Crop Protection, 31(1), 78-84. https://doi.org/10.1016/j.cropro.2011.10.004

Gil, E., Campos, J., Ortega, P., Llop, J., Gras, A., Armengol, E., Salcedo, R., Gallart, M., 2019. DOSAVIÑA: Tool to calculate the optimal volume rate and pesticide amount in vineyard spray applications based on a modified leaf wall area method. Computers and Electronics in Agriculture, 160, 117-130. https://doi.org/10.1016/j.compag.2019.03.018

Hurvich, C. M., Tsai, C. L., 1993. A corrected Akaike information criterion for vector autoregressive model selection. Journal of Time Series Analysis, 14(3), 271-279. https://doi.org/10.1111/j.1467-9892.1993.tb00144.x

Koch, H., 1993. Application rate and spray deposit on targets in plants. In: ANPP/BCPC 2nd International Symposium on Pesticides Applications, Strasbourg, France, 1, 175–182.

Llorens, J., Gil, E., Llop, J., Escolà, A., 2010. Variable rate dosing in precision viticulture: Use of electronic devices to improve application efficiency. Crop Protection, 29(3), 239-248. https://doi.org/10.1016/j.cropro.2009.12.022

Llorens, J., Gil, E., Llop, J., Escolà, A., 2011a. Ultrasonic and LiDAR Sensors for Electronic Canopy Characterization in Vineyards: Advances to Improve Pesticide Application Methods. Sensors, 11(2), 2177-2194. https://doi.org/10.3390/s110202177

Llorens, J., Gil, E., Llop, J., Queraltó, M., 2011b. Georeferenced LiDAR 3D Vine Plantation Map Generation. Sensors, 11(6), 6237-6256. https://doi.org/10.3390/s110606237

677 Lorenz, D. H., Eichorn, K. W., Bleiholder, H., Klose, U., Meier, U., Weber, E., 1994. Phänologische
678 Entwicklungsstadien der Weinrebe (Vitis vinifera L. spp. Vinifera). (Phenological stages of
679 grapevine (Vitis vinifera L. spp. Vinifera)). Viticultural and Enological Science 49, 66-70.
680 https://doi.org/10.1111/j.1755-0238.1995.tb00085.x
681 Moorthy, I., Miller, J. R., Berni, J. A. J., Zarco-Tejada, P., Hu, B., Chen, J., 2011. Field
682 characterization of olive (Olea europaea L.) tree crown architecture using terrestrial laser scanning
683 data. Agricultural and Forest Meteorology, 151(2), 204-214.
684 https://doi.org/10.1016/j.agrformet.2010.10.005
685 Palleja, T., Landers, A. J., 2015. Real time canopy density estimation using ultrasonic envelope signals
686 in the orchard and vineyard. Computers and Electronics in Agriculture, 115, 108-117.
687 http://dx.doi.org/10.1016/j.compag.2015.05.014
688 Pergher, G., Petris, R., 2008. Pesticide dose adjustment in vineyard spraying and potential for dose
689 reduction. Manuscript ALNARP 08 011. Agricultural Engineering International CIGR Journal, 10,
690 1-9.
691 R Core Team., 2020. R: A language and environment for statistical computing. R Foundation for
692 Statistical Computing, Vienna, Austria. URL http://www.R-project.org/
693 Rosell, J. R., Llorens, J., Sanz, R., Arnó, J., Ribes-Dasi, M., Masip, J., Escolà, A., Camp, F.,
694 Solanelles, F., Gràcia, F., Gil, E., Val, L., Planas, S., Palacín, J., 2009. Obtaining the three-
695 dimensional structure of tree orchards from remote 2D terrestrial LiDAR scanning. Agricultural
696 and Forest Meteorology, 149(9), 1505-1515. https://doi.org/10.1016/j.agrformet.2009.04.008
697 Rosell, J.R., Sanz, R., 2012. A review of methods and applications of the geometric characterization of
698 tree crops in agricultural activities. Computers and Electronics in Agriculture, 81, 124-141.
699 https://doi.org/10.1016/j.compag.2011.09.007
700 Rüegg, J., Siegfried, W., Raisigl, U., Viret, O., Steffek, R., Reisenzein, H., Persen, U., 2001.
701 Registration of plant protection products in EPPO countries: Current status and possible approaches
702 to harmonization. EPPO Bulletin, 31(2), 143-152. https://doi.org/10.1111/j.1365-
703 2338.2001.tb00983.x

Siegfried, W., Viret, O., Huber, B., Wohlhauser, R., 2007. Dosage of plant protection products adapted to leaf area index in viticulture. Crop Protection, 26(2), 73-82. https://doi.org/10.1016/j.cropro.2006.04.002

Solanelles, F., Escolà, A., Planas, S., Rosell, J. R., Camp, F., Gràcia, F., 2006. An Electronic Control System for Pesticide Application Proportional to the Canopy Width of Tree Crops. Biosystems Engineering, 95(4), 473-481. https://doi.org/10.1016/j.biosystemseng.2006.08.004

Vivier, M. A., Pretorius, I. S., 2002. Genetically tailored grapevines for the wine industry. Trends in Biotechnology, 20(11), 472-478. https://doi.org/10.1016/S0167-7799(02)02058-9

Walklate, P. J., Cross, J. V., Richardson, G. M., Murray, R. A., Baker, D. E., 2002. Comparison of different spray volume deposition models using LIDAR measurements of apple orchards. Biosystems Engineering, 82 (3), 253–267. https://doi.org/10.1006/bioe.2002.0082

Walklate, P. J., Cross, J.V., Pergher, G., 2011. Support system for efficient dosage of orchard and vineyard spraying products. Computers and Electronics in Agriculture 75, 355–362. https://doi.org/10.1016/j.compag.2010.12.015

Walklate, P. J., Cross, J. V., 2012. An examination of Leaf-Wall-Area dose expression. Crop Protection, 35, 132-134. https://doi.org/10.1016/j.cropro.2011.08.018

Figures caption

Figure 1. Empirical density curves of deposition values as a function of spray date (T1, T2, T3, T4) obtained from 2017 calibration data.

Figure 2. Evolution of primary canopy attributes VH (A), VW (B) and IBR (C) at the vine trio scale (shown as a dot on graphs) by blocks (Aranel (red), Caladoc (brown), Marselan (green), Petit verdot (blue) and Syrah (purple)) over the entire growing season (T1 to T4) in 2017. At each date, a box plot is presented in order to summarise the information obtained for the relevant primary canopy attribute.

731 Figure 3. Relationship between the median deposition observed in 2016 and the median deposition in
732 2016 predicted from of univariate models for prediction of median deposition calibrated in 2017 on
733 the Collection, Faysse, Franquet and Petit Verdot blocks over the entire growing season (T1 red
734 square, T2 green triangle, T3 blue dot and T4 purple cross), coefficient of determination (R^2) of 0.79,
735 normalised root mean square error of prediction (nRMSEp) of 30% and bias of + 2.0%. The black
736 curve represents a 1:1 linear curve.
737
738 Figure 4. a: Relationship between the median deposition observed in 2016 and the median deposition
739 predicted from multivariate models for prediction of median deposition calibrated in 2017 (T1 red
740 square, T2 green triangle, T3 blue dot and T4 purple cross), R^2 = 0.94, nRMSE = 13% and bias = -
741 2.1%. The black curve represents a 1:1 linear fit.
742 b: Evolution of D5 median spray deposits as a linear combination of primary canopy attributes
743 measured over the entire field and growing season (T1 red square, T2 green triangle, T3 blue dot and
744 T4 purple cross) in 2017. The dotted black curve represents the multivariate model for prediction of
745 median deposition (see D5 in Table 6 for parameters and statistics).
746

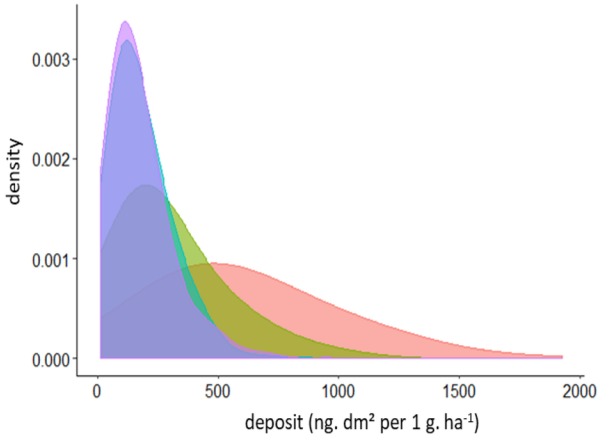
density
0.003
0.002
0.001
0.000
0
500
1000
1500
2000
deposit (ng. dm² per 1 g. ha-1)

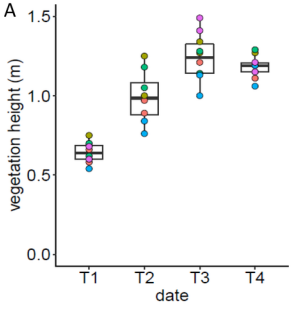
A
vegetation height (m)
1.5
1.0
0.5
0.0
T1
T2
T3
T4
date

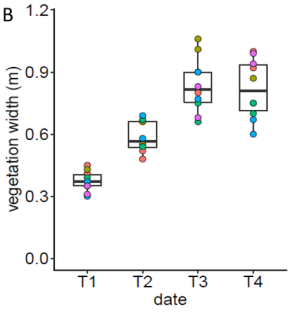
B
vegetation width (m)
1.2
0.9
0.6
0.3
0.0
T1
T2
T3
T4
date

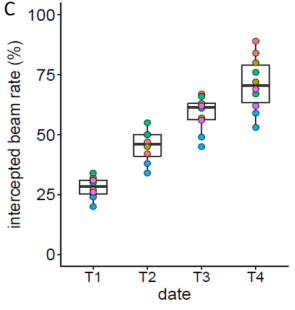
C
intercepted beam rate (%)
100
75
50
25
0
T1
T2
T3
T4
date

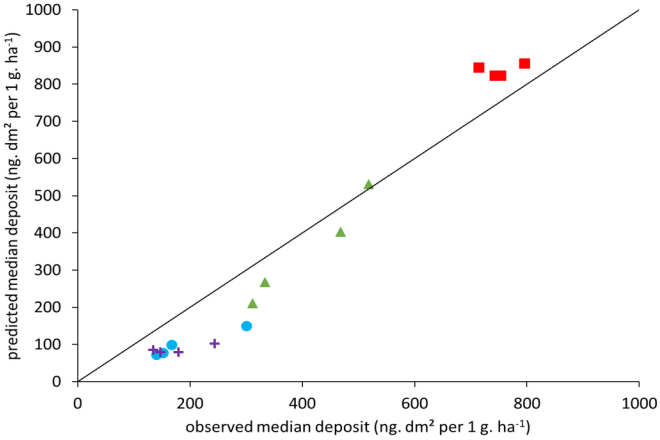
predicted median deposit (ng. dm² per 1 g. ha⁻¹)
observed median deposit (ng. dm² per 1 g. ha⁻¹)
0
100
200
300
400
500
600
700
800
900
1000

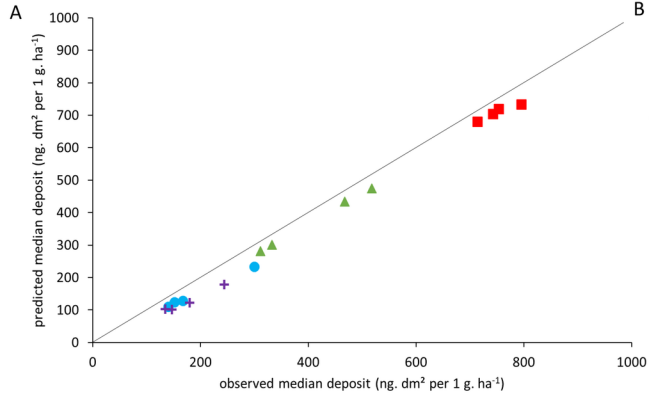
A
predicted median deposit (ng. dm² per 1 g. ha⁻¹)
observed median deposit (ng. dm² per 1 g. ha⁻¹)
0
200
400
600
800
1000
100
300
500
700
900

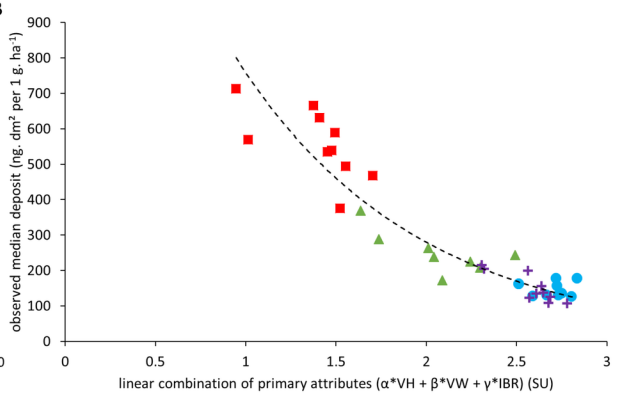
B
observed median deposit (ng. dm² per 1 g. ha⁻¹)
linear combination of primary attributes (α*VH + β*VW + γ*IBR) (SU)
0
0.5
1
1.5
2
2.5
3
100
200
300
400
500
600
700
800
900

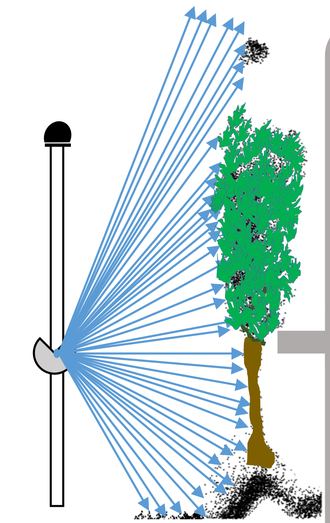

Database of geo-referenced point clouds

Primary canopy attributes

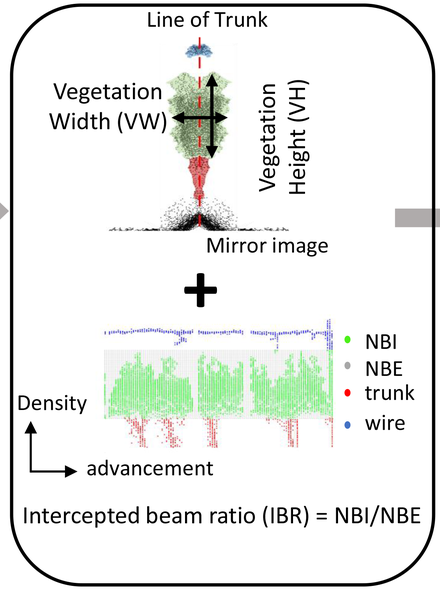

Aggregated canopy indicator (reference method)

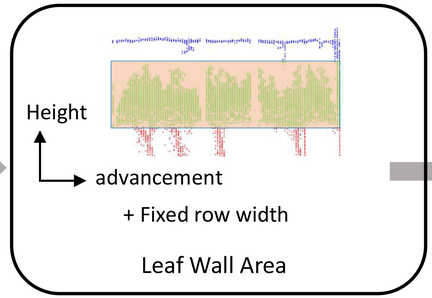

Calibration step

Multivariate model with canopy attributes

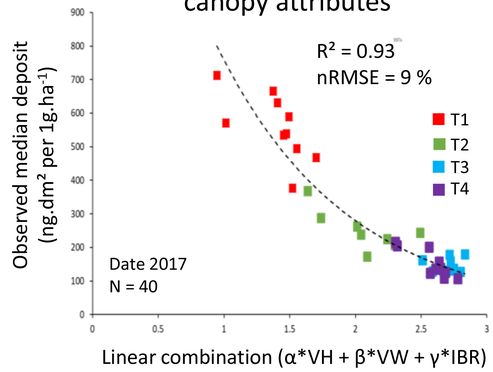

T1 = early season, T2 = early-mid season,
T3 = mid season, T4 = mid-late season

Univariate model with aggregated canopy indicator

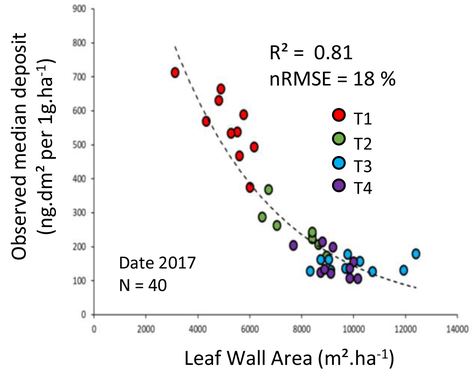

Spray deposition model quality (Validation data set)

Date 2016
N = 16

Multivariate model of decile depositions

Multivariate model of median deposition

Univariate model of median deposition

Increasing model quality
Decreasing model uncertainty

LiDAR generates local canopy dimensions. 1° canopy dimensions are better predictors than the current reference aggregated indicator and, modelling spray deposition distributions instead of the median improved deposition prediction models.